

The barrier functions of crude cervical mucus plugs against HIV-1 infection in the context of cell-free and cell-to-cell transmission

Baxolele Mhlelude^{a,b,c,d}, Annasara Lenman^b, Phikolomzi Sidoyi^h, Jim Joseph^j, Jochen Kruppa^g, Charles Bitamazire Busingeⁱ, Mana Lungisa Mdakaⁱ, Frank Konietzschke^{d,g}, Andreas Pich^f, Gisa Gerold^{b,e,k}, Christine Goffinet^{b,c,d,*} and Anwar Suleman Mall^{a,*}

Objective: The cervical mucus plugs are enriched with proteins of known immunological functions. We aimed to characterize the anti-HIV-1 activity of the cervical mucus plugs against a panel of different HIV-1 strains in the contexts of cell-free and cell-associated virus.

Design: A cohort of consenting HIV-1-negative and HIV-1-positive pregnant women in labour was recruited from Mthatha General Hospital in the Eastern Cape province of South Africa, from whom the cervical mucus plugs were collected in 6 M guanidinium chloride with protease inhibitors and transported to our laboratories at -80°C .

Methods: Samples were centrifuged to remove insoluble material and dialysed before freeze-drying and subjecting them to the cell viability assays. The antiviral activities of the samples were studied using luminometric reporter assays and flow cytometry. Time-of-addition and BlaM-Vpr virus-cell fusion assays were used to pin-point the antiviral mechanisms of the cervical mucus plugs, before proteomic profiling using liquid chromatography-tandem mass spectrometry.

Results: The proteinaceous fraction of the cervical mucus plugs exhibited anti-HIV-1 activity with inter-individual variations and some degree of specificity among different HIV-1 strains. Cell-associated HIV-1 was less susceptible to inhibition by the potent samples whenever compared with the cell-free HIV-1. The samples with high antiviral potency exhibited a distinct proteomic profile when compared with the less potent samples.

Conclusion: The crude cervical mucus plugs exhibit anti-HIV-1 activity, which is defined by a specific proteomic profile.

Copyright © 2021 The Author(s). Published by Wolters Kluwer Health, Inc.

AIDS 2021, **35**:2105–2117

Keywords: cervical mucus plugs, HIV-1, mucins

^aUniversity of Cape Town, Department of Surgery, Groote Schuur Hospital, Observatory, South Africa, ^bTWINCORE, Centre for Experimental and Clinical Infection Research; a joint venture between the Hannover Medical School and the Helmholtz Centre for Infection Research, Institute of Experimental Virology, Hannover, ^cCharité – Universitätsmedizin Berlin, Institute of Virology, Charité Campus Mitte, ^dBerlin Institute of Health, Berlin, Germany, ^eUmeå University, Department of Clinical Microbiology, Virology & Wallenberg Centre for Molecular Medicine (WCMM), Umeå, Sweden, ^fHannover Medical School, Institute of Toxicology, Core Facility Proteomics, Hannover, ^gCharité – Universitätsmedizin Berlin, Institut für Biometrie und Klinische Epidemiologie, Charité Campus Mitte, Berlin, Germany, ^hFaculty of Health Sciences, School of Medicine, Walter Sisulu University, Mthatha, South Africa, ⁱDepartment of Obstetrics and Gynaecology, Walter Sisulu University/Nelson Mandela Academic Hospital, ^jDepartment of Human Biology, Walter Sisulu University, Mthatha, South Africa, and ^kDepartment of Biochemistry, University of Veterinary Medicine Hannover, Hanover, Germany.

Correspondence to Anwar Suleman Mall, Department of Surgery, Faculty of Health Sciences, University of Cape Town, 7925 Observatory, Cape Town, South Africa.

Tel: +27 21 7869465; e-mail: anwar.mall@uct.ac.za

* Christine Goffinet and Anwar Suleman Mall contributed equally to the study design, experimentation, supervision, data analysis and writing of this article.

Received: 4 February 2021; revised: 7 May 2021; accepted: 31 May 2021.

DOI:10.1097/QAD.0000000000003003

ISSN 0269-9370 Copyright © 2021 The Author(s). Published by Wolters Kluwer Health, Inc. This is an open access article distributed under the terms of the Creative Commons Attribution-Non Commercial-No Derivatives License 4.0 (CCBY-NC-ND), where it is permissible to download and share the work provided it is properly cited. The work cannot be changed in any way or used commercially without permission from the journal.

Introduction

Mucosal surfaces lining the internal tracts of the body are vulnerable to damage by exogenous factors mostly through air and food intake [1–4]. A thin layer of mucus gel lines the various mucosae, regulates access of exogenous factors into the underlying epithelia, and protects against its desiccation [1]. Crude mucus consists of mucins, nonmucin proteins, lipids, water (95–97%) and cell debris [1,2]. Mucins are a large family of heavily glycosylated proteins of high molecular weight (0.5–20 MDa), which are either membrane-bound or secreted as gel-forming and non-gel-forming, depending on their ability to polymerize and crosslink into a gel [1]. Their genes have been mapped on several chromosomes across the human genome [3]. Crude saliva, its purified mucins [4] and mucins purified from breast milk [5] inhibit HIV-1 in *in-vitro* assays.

The cervix produces ~60 mg of mucus per day, the viscosity of which changes periodically with fluctuating levels of oestrogen and progesterone [6], thus regulating access of the spermatozoa into the uterus. Mucus is receptive or resistant during the oestrogen-dominant or progesterone-dominant phases, respectively, with the latter phase blocking access into the uterus [7]. Antimicrobials in the cervical mucus strengthen its barrier functions against invading pathogens [8,9], whereas the constant mucus turnover ensures their clearance from the female reproductive tract (FRT) [10]. During the early stages of pregnancy, increasing progesterone levels drive the formation of the cervical mucus plug (CMP) in the cervix, which blocks bacterial entry into the uterus, failure of which may cause life-threatening obstetrical problems [11,12].

The secreted gel-forming mucins – MUC5AC, MUC5B and MUC6 – make up the cervical mucus [13,14] and are encoded by a gene cluster (~500 kb) that is located on chromosome 11p15.5 together with *MUC2* [1], the expression of which in the cervix is controversial [13]. Lying underneath the cervical mucus layer is a glycocalyx, which is predominantly attributed to the membrane-bound mucins: MUC1, MUC4 and MUC16 [13,14]. They block pathogens from invading the underlying epithelium, and signal underlying immune cells to trigger an immune response against invading pathogens [15,16]. The expression levels of *MUC4* and *MUC5B* transcripts are high in the cervix [17], the latter peaking at mid-cycle [18].

Given the enrichment of the CMPs with antimicrobial factors [8,9,19], we investigated whether the CMP and its mucin components had anti-HIV-1 activity *in vitro*. We probed samples against a panel of replication-competent SIV and HIV-1 strains in the contexts of cell-free and cell-to-cell infections. We found that the CMPs inhibit HIV-1 more potently than the purified mucins, and exhibit a viral tropism-specific sieve effect and heterogeneity in terms of their antiviral mechanisms and potency, possibly driven by a specific proteomic profile.

Methods

Ethics statement

This study was approved by the Human Research Ethics Committee of the University of Cape Town (HREC REF: 102/2013) and the provincial health department of the Eastern Cape (EC_2016RP7_393). The CMPs were collected with strict adherence to the principles expressed in the Declaration of Helsinki [20].

Recruitment of participants and sample collection

Fifty-two pregnant women were recruited from the maternity unit of Mthatha General Hospital, Eastern Cape, South Africa; between October 2016 and April 2017. The CMPs were collected in 6M guanidinium hydrochloride (GuHCl) (Sigma, Kempton Park, South Africa) with protease inhibitors [21], following spontaneous shedding or retrieval during labour.

Preparation of the cervical mucus plugs and purification of the cervical mucins

The CMPs were prepared as previously described [21]. Mucins were purified by caesium chloride (CsCl) density gradient ultracentrifugation and Sepharose CL-2B gel filtration [22]. Samples were adjusted to a density of 1.4 g/ml with CsCl (Sigma) and 4 M GuHCl (Sigma), and centrifuged (70Ti rotor) at 40 000 rpm for 48 h at 4 °C in a Beckman Optimal L-80 XP Ultracentrifuge (Beckman Coulter, South Africa). Fractionated samples were analysed for their protein and glycoprotein content using Bradford and Periodic Acid Schiff (PAS) assays, respectively. The glycoprotein-rich fractions were pooled and subjected to gel filtration [23], followed by pooling of the V_0 and V_i fractions. All samples were dialyzed against three changes of distilled water and freeze-dried in a Labconco (USA) Freeze Dryer.

Sodium dodecyl sulphate polyacrylamide gel electrophoresis

Samples (100 µg) were reconstituted in 1× SDS buffer and resolved on 4–20% gradient sodium dodecyl sulphate PAGE (SDS-PAGE) [24]. The gels were stained separately with Vacutec Aqua Stain (Vacutec, South Africa) and PAS (Sigma) for proteins and glycoproteins, respectively.

Immunoblotting

After SDS-PAGE, samples were electro-blotted on to nitrocellulose membranes using the SV20-SDB system (Sigma, UK), and subjected to western blot analysis as previously described [21].

Cell culture and transfections

Unless stated otherwise, HEK293T and TZM-bl cells were cultured in Dulbecco's Modified Eagle's Medium (DMEM) (Sigma, UK) supplemented with 10% foetal bovine serum (Sigma, UK), 100 units/ml penicillin (Gibco, UK), 100 µg/ml streptomycin and 2 mmol/l L-glutamine (Gibco, UK).

PM1 and parental Jurkat T cells were cultured in Roswell Park Memorial Institute (RPMI) 1640 medium (Sigma, UK) with the same supplements as mentioned above. Transfections were performed using CalPhos Mammalian Transfection Kit (Takara, Frankfurt-am-Main, Germany). All cell lines were cultured at 37 °C/5% CO₂.

Cell viability assays

Samples were reconstituted in 10% DMEM to a final concentration of 1 mg/ml. TZM-bl cells were treated with samples for 48 h. 10% SDS (Sigma, Germany) in 1 N HCl (Sigma, Germany) was used as a positive control to induce toxicity. Posttreatment, cells were subjected to cell viability assays using CellTiter Glo Luminescent Cell Viability Assay Kit (Promega, Germany).

Virus stocks production and titration

HEK293T cells were transfected with pro-viral DNA encoding either full length SIV_{mac239} or HIV-1 strains [25,26]. Production of β -lactamase (BlaM)-carrying HIV-1 was conducted by triple transfection of HEK293T cells with pYU-2/pNL4.3 (60 μ g), pBlaM (20 μ g) and pAdvantage (8 μ g) [27,28]. Forty-eight-hour posttransfection, virus-containing culture supernatants were concentrated on a 20% sucrose cushion [25] and titrated on TZM-bl cells using β -galactosidase-based blue cell assay [25]. HIV-1_{Ba-L} was obtained from the NIH AIDS reagent (USA), propagated in PM1 cells [29] and titrated as mentioned above [25].

Luciferase assays

TZM-bl cells were inoculated for 48 h with individual virus stocks treated with two-fold serially diluted samples for 1 h at 37 °C. Postinfection, cells were subjected to luciferase assays using the Luciferase Assay System (Promega, Germany).

Time-of-addition assays

For pretreatment, TZM-bl cells were incubated with the CMPs for 1 h at 37 °C, followed by sample removal prior to infection with HIV-1. For posttreatment, cells were infected with HIV-1 for 1 h prior to treatment with the CMPs at 1:2 ratio. For co-treatment, HIV-1 was incubated with the CMPs at 1:2 ratio for 1 h prior to infection. 48 h postinfection, cell lysates were subjected to luminometric luciferase assays.

β -lactamase fusion assays

The BlaM-carrying HIV-1 strains were incubated with the samples for 1 h, before infecting TZM-bl cells for 4 h. Maraviroc (25 μ mol/l) and T20 (50 μ mol/l) were used as inhibitors of viral entry and fusion, respectively. The CCF4 spectral shift was analysed using a multiparameter LSRII flow cytometry with DIVA software (BD Biosciences, Germany).

Green fluorescent protein-based cell-free and cell-to-cell infection assays

Cell-free HIV-1_{NL4.3-GFP} [25] was incubated with the CMPs (1 mg/ml) for 1 h at 1:2 ratio, before infecting

Jurkat T cells for 48 h. To model cell-to-cell transmission, HEK293T cells were transfected with pro-viral DNA encoding full length HIV-1_{NL4.3-GFP} followed by a medium change after 4 h and incubation for 24 h. On the next day, virus-producing cells were treated (1:2 ratio) with 1 mg/ml of the CMPs for 1 h and co-cultured with Jurkat T cells for 24 h. These experiments were conducted in the absence or presence of efavirenz (100 nmol/l). Postinfection, green fluorescent protein (GFP) expression was quantified using a BD FACSCalibur flow cytometer (BD Biosciences, Germany).

In-gel protein digestion and liquid chromatography-mass spectrometry/mass spectrometry analysis of the cervical mucus plugs

The CMPs (100 μ g) were reconstituted in 1 \times SDS buffer and boiled at 95 °C for 5 min. Samples were then alkylated by adding acrylamide to a final concentration of 2%, resolved on 7.5% linear SDS-PAGE [24] and stained with Bio-Safe Coomassie Stain (Bio-Rad, Germany). The in-gel digestion and liquid chromatography coupled with tandem mass spectrometry were conducted as described elsewhere [30].

Bioinformatics analysis

Raw data from mass spectrometry were processed using MaxQuant [31], and human UniProt/SwissProt entries containing common contaminants. Proteins were identified by a false discovery rate of 0.01 on protein and peptide level, and quantified by extracted ion chromatograms of all peptides. The processed data were analysed using Perseus v1.6.0.7. Missing values were imputed from normal distribution (width, 0.3; down shift, 1.8). Statistical analysis was performed using two-sample *t* test, by comparing LFQ intensities of proteins in the HIV-1-positive cohort against the HIV-1-negative cohort [false discovery rate (FDR), 0.5; *s*₀, 0.1], and group 1 against group 2 (FDR, 0.36; *s*₀, 0.1). STRING [32] and functional enrichment analysis were performed on 116 proteins enriched in group 1.

Statistical analysis

One-way ANOVA and student *t* test were used to compare the means, whereby the error bars represent mean and standard deviation (*m* \pm SD). Statistical analysis was conducted using GraphPad Prism v5 (La Jolla, California, USA), and a *P* value of 0.05 or less was considered significant. The flow cytometry data were analysed using FlowJo v10 (Tree Star, Ashland, Oregon, USA).

Results

Anti-HIV-1 activities of the cervical mucus plugs and purified mucins in the context of cell-free infection

We purified mucins from the CMPs collected from HIV-1-negative and HIV-1-positive pregnant women in

labour [22] (clinical information in Supplementary Table 1, <http://links.lww.com/QAD/C220>). Purification profiles between samples were comparable, irrespective of the donor's HIV-1 status (Supplementary Fig. 1a and b, <http://links.lww.com/QAD/C221>). Samples varied in terms of their electrophoretic patterns within each cohort (Supplementary Fig. 1c–f, <http://links.lww.com/QAD/C221>). MUC5AC and MUC5B were generally detectable by immunoblotting among the CMPs (Supplementary Fig. 1g and h, <http://links.lww.com/QAD/C221>) and purified mucins (Supplementary Fig. 1i and j, <http://links.lww.com/QAD/C221>), with varying levels of expression between the individual samples, independent of the donor's HIV-1 status. TZM-bl cells treated with 1 mg of CMPs or purified mucins maintained their viability (Supplementary Fig. 2, <http://links.lww.com/QAD/C222>), suggesting no potential toxicity.

The CMPs from both cohorts exhibited antiviral activity against SIV and HIV-1 strains, independent of the viral tropism (Fig. 1a and b). This varied between and within individual samples, with certain samples (5, 18, 32, 39 and 47) showing both antiviral and pro-viral activities, depending on the infecting strain. Generally, the CMPs robustly inhibited HIV-1_{NL4.3}, while there was a high level of heterogeneity for inhibition of HIV-1_{Ba-L}. SIV_{mac239} displayed sensitivity to low-dosed CMPs and resistance to increasing CMP concentration. We used area under the curve (AUC) to measure viral sensitivity to the samples [33,34]. Using the cumulative AUCs from all tests, we found that samples from the HIV-1-positive cohort were more potent than those from the HIV-1-negative cohort (Fig. 1c). Furthermore, the X4-tropic strains of HIV-1 were more susceptible to inhibition than the R5-tropic HIV-1 strains (Fig. 1d).

Purified cervical mucins inhibited HIV-1 in a dose-dependent fashion, irrespective of the donor's HIV-1 status and viral tropism (Supplementary Fig. 3a and b, <http://links.lww.com/QAD/C223>). Unlike the CMPs (Fig. 1a and b), purified mucins showed a consistent antiviral activity against both HIV-1 strains. Similar to the CMPs, purified mucins from the HIV-1-positive cohort were more potent than those from the HIV-1-negative cohort (Supplementary Fig. 3c, <http://links.lww.com/QAD/C223>). However, in contrast to the CMPs, the R5-tropic HIV-1_{Ba-L} was more susceptible to inhibition by the purified mucins compared with the X4-tropic HIV-1_{NL4.3} (Supplementary Fig. 3d, <http://links.lww.com/QAD/C223>).

Mechanism(s) behind the anti-HIV-1 activities of the cervical mucus plugs in the context of cell-free infection

We investigated the possible mechanism(s) behind the heterogeneous anti-HIV-1 activities of the CMPs by time-of-addition assays (Fig. 2a). Treating the virus stocks with the CMPs before incubation with TZM-bl cells (co-

treatment) showed the most potent antiviral activity, regardless of the donor's HIV-1 status (Fig. 2b). Addition of the CMPs to cells 1 h after (posttreatment) and before (pretreatment) HIV-1 infection showed reduced inhibition. Overall, the CMPs were inhibitory against HIV-1 across all three conditions when compared with the virus-only control, and their activity is largely virus-directed, and not or to a lesser extent cell-directed. To investigate if the anti-HIV-1 activity of the CMPs and mucins involves inhibition of virus entry and fusion, we subjected samples to BlaM-Vpr-based fusion assays. Despite their universal antiviral activity against HIV-1_{YU-2} and HIV-1_{NL4.3} (Fig. 1), not all tested CMPs (Fig. 2c–f) inhibited virus cell fusion, suggesting that some samples exert postentry anti-HIV-1 activities. Purified mucins showed a mild to no inhibition of fusion (Supplementary Fig. 4, <http://links.lww.com/QAD/C224>).

Anti-HIV-1 activities of the cervical mucus plugs in the context of cell-to-cell transmission

HIV-1 can infect target cells through cell-free and cell-to-cell transmission, with the latter mode being the most effective one through which HIV-1 spreads *in vivo* [35,36]. We investigated the effect of the CMPs on HIV-1 infection of Jurkat T cells (Fig. 3) in cell-free and cell-to-cell transmission.

In agreement with the luciferase assays (Fig. 1), the CMPs displayed potent anti-HIV-1_{NL4.3-GFP} activity in cell-free infection (Fig. 3a and b), which varied in potency between samples, independent of the donor's HIV status. The CMPs also inhibited HIV-1_{NL4.3-GFP} in cell-to-cell transmission, albeit to a lesser extent than cell-free infection (Fig. 3c and d). In both conditions, inhibition was more pronounced in the presence of efavirenz. These results suggest that HIV-1_{NL4.3-GFP} partially overcame the barrier functions of the CMPs in the context of cell-to-cell transmission compared with cell-free infection (Fig. 3e) [35].

Liquid chromatography-mass spectrometry/mass spectrometry -based proteomic profiling of the cervical mucus plugs

We then investigated the proteomic profiles of the CMPs by SDS-PAGE and label-free quantitative (LFQ) mass spectrometry. Bio-Safe Coomassie Stain intensified with decreasing molecular weight of the protein species (Fig. 4a). Statistical comparison of the abundance of the CMP proteins between HIV-1-negative and HIV-1-positive cohorts (Supplementary Data File 1, <http://links.lww.com/QAD/C227>) showed 71 proteins that were significantly upregulated in the HIV-1-positive cohort, amongst which were MUC1, MUC5AC and MUC6 (Fig. 4b). Several pregnancy-specific glycoproteins (PSGs), protein S and MUC21 were amongst the significantly downregulated 17 proteins in the same cohort. An unsupervised hierarchical clustered heatmap of 88 differentially expressed proteins showed distinct

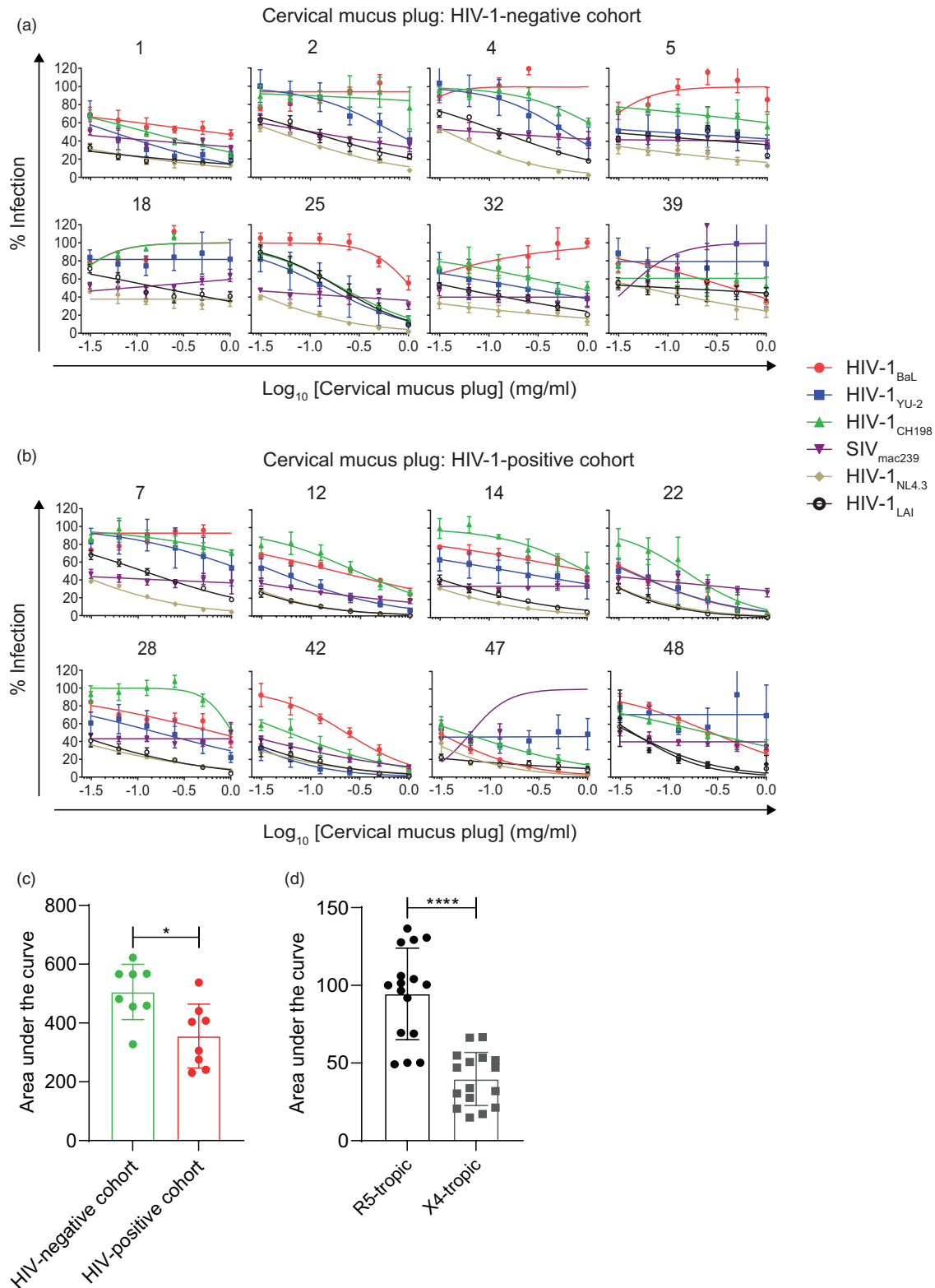


Fig. 1. Anti-HIV-1 activity of the cervical mucus plugs. Dose–response curves showing the activity of the CMPs from the (a) HIV-1-negative and (b) HIV-1-positive cohort against indicated strains of HIV-1 and SIV. One-way analysis of variance (ANOVA) was used to compare the means. Error bars represent the SD of duplicates from three experiments. Bar graphs showing the antiviral potencies of the CMPs based on the donor's (c) HIV-1 status and (d) viral tropism, following evaluation of the cumulative area under the curve (AUC) arithmetic means by the unpaired and paired student *t* tests, respectively, between the groups. The error bars represent the SD. CMPs, cervical mucus plugs.

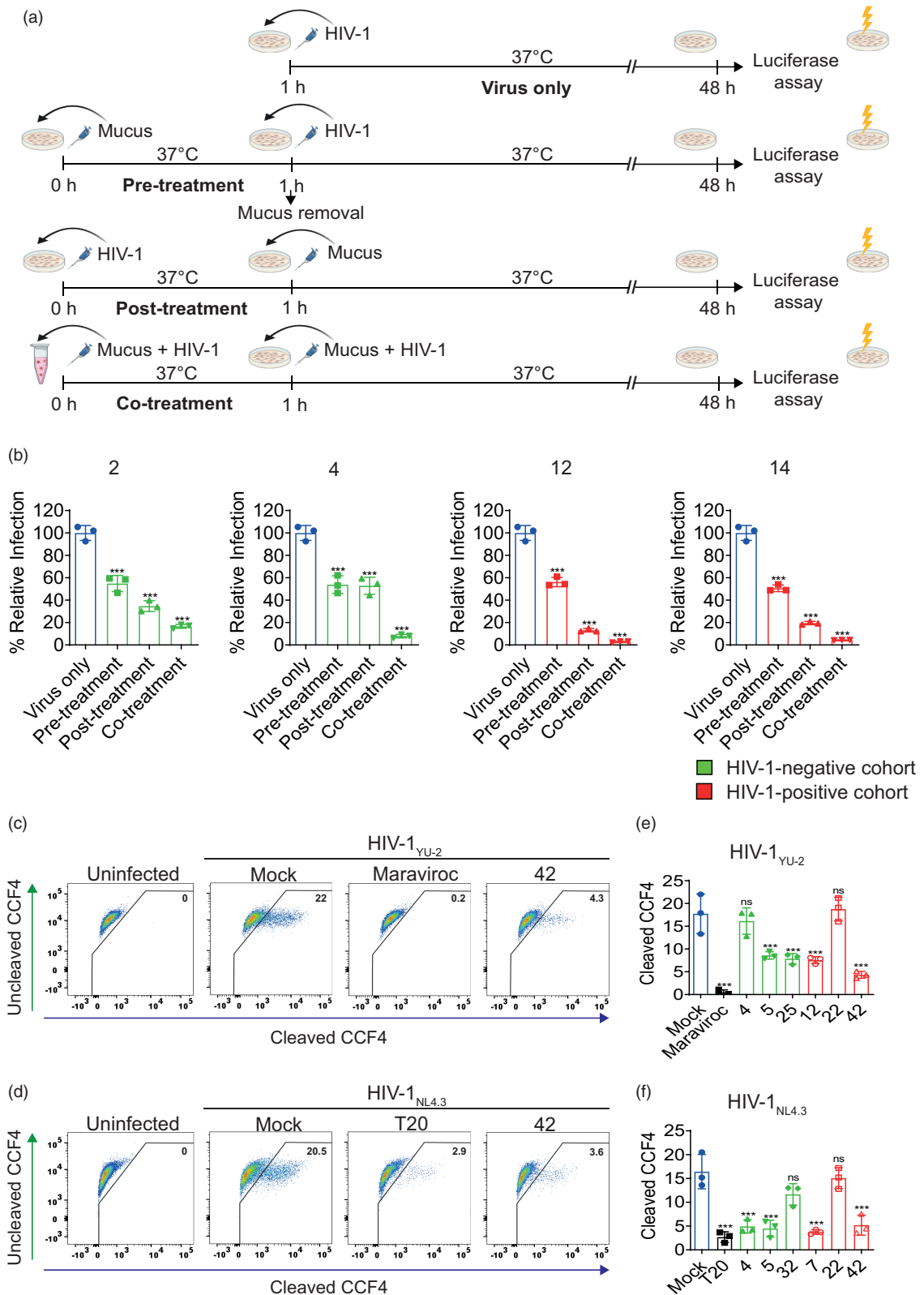


Fig. 2. Probing the mechanisms behind the anti-HIV-1 activity of the cervical mucus plugs. (a) Schematic diagram showing the experimental set up of the time-of-addition assays. (b) Luminometric measurement of relative infection. Representative FACS dot plots showing fusion inhibition of BlaM-Vpr-positive (c) HIV-1_{YU-1} and (d) HIV-1_{NL4.3}. (e and f) The FACS data were quantified and presented in the form of bar graphs, respectively. Bar graphs indicate arithmetic means. Error bars represent SD from three experiments. CMPs, cervical mucus plugs.

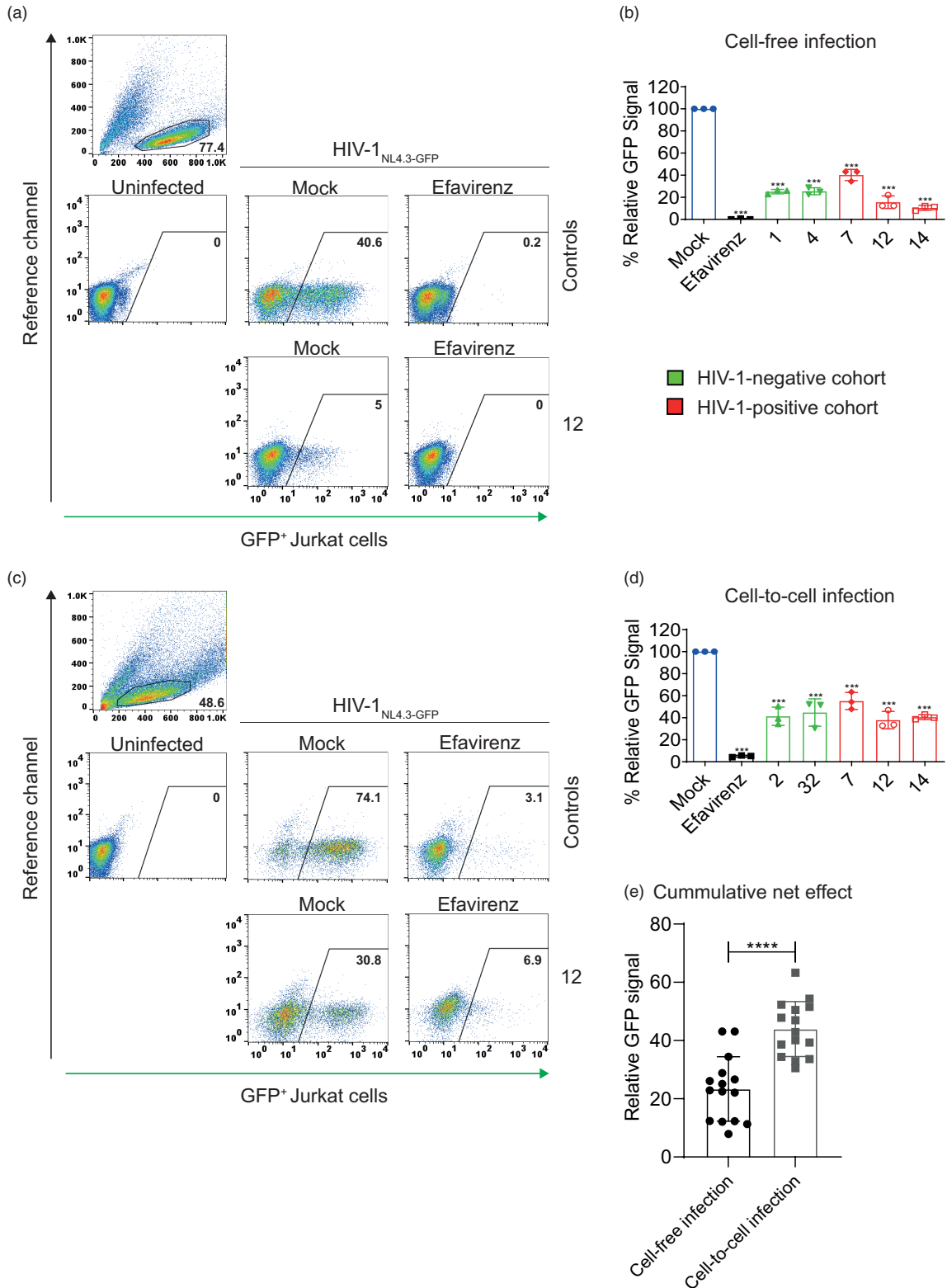


Fig. 3. Antiviral activity of the cervical mucus plugs against HIV-1 strains in the context of cell-to-cell infection. Representative FACS dot plots showing the antiviral activity of the CMPs in the contexts of (a) cell-free and (c) cell-to-cell infections. The FACS data from (b) cell-free and (d) cell-to-cell infection assays were quantified and presented as the bar graphs. One-way analysis of variance (ANOVA) was used to compare the means, where the error bars represent the SD from three experiments. (e) Bar graphs showing a comparison of the cumulative net effects from cell-free and cell-to-cell infection assays. Paired student *t* test was used to compare the means, where the error bars represent the SD from three experiments. CMPs, cervical mucus plugs.

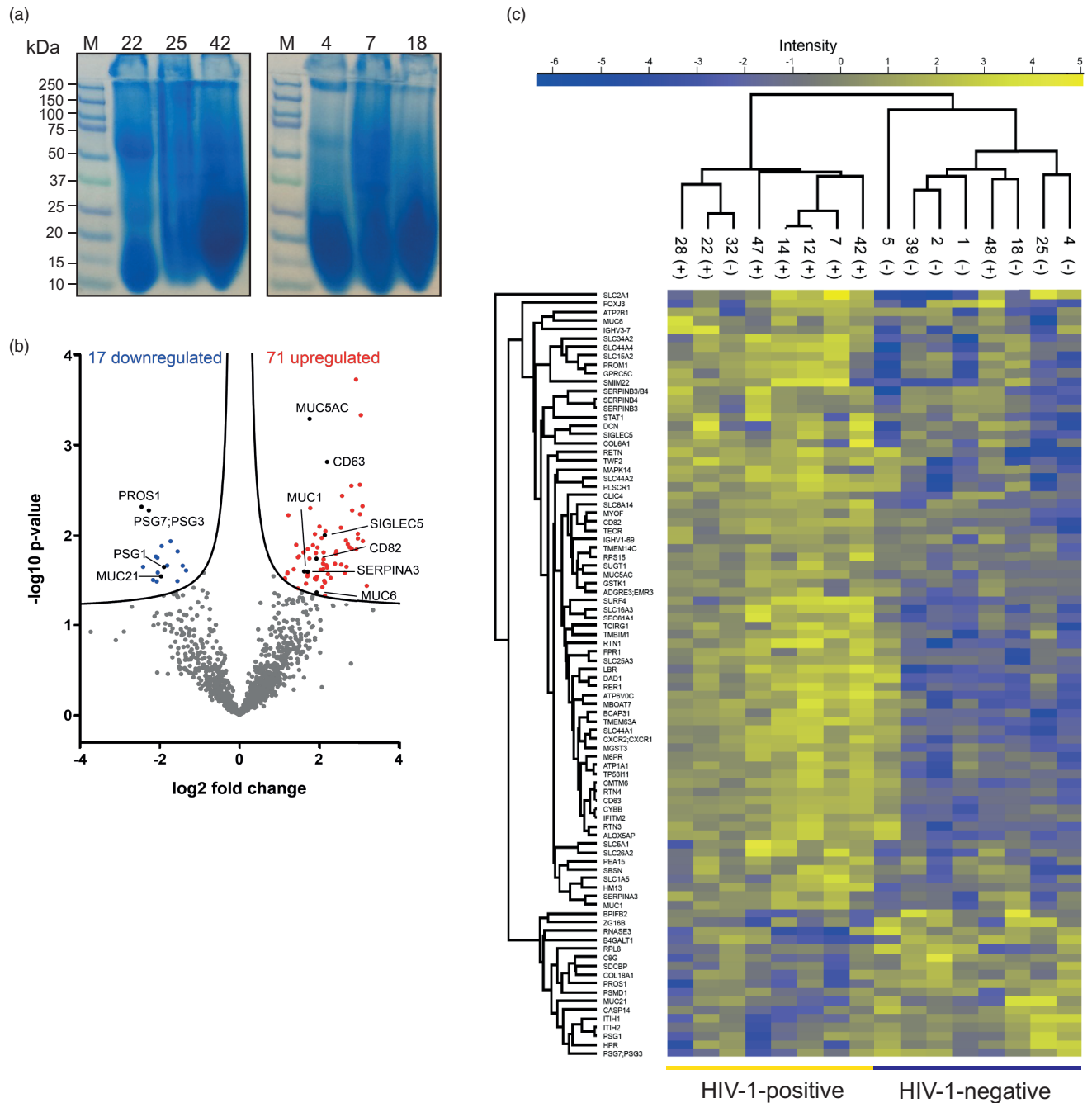


Fig. 4. Proteomic profiling of the cervical mucus plugs from the HIV-1-negative and HIV-1-positive cohorts. (a) Analysis of the CMPs on 7.5% linear SDS-PAGE following staining with Bio-Safe Coomassie staining. (b) Volcano plot showing significantly upregulated (71) and downregulated (17) proteins between the two cohorts. The statistical P value ($-\log_{10} P$) is plotted against the LFQ intensity difference (\log_2). (c) Heatmap showing the significantly regulated proteins in the CMPs collected from HIV-1-negative and HIV-1-positive cohorts following an unsupervised hierarchical clustering. CMPs, cervical mucus plugs.

proteomic profiles between the two cohorts, with the exception of two outliers (samples 32 and 48), which exhibited different proteomic profiles from those in their respective cohorts (Fig. 4c).

As the donor's HIV-1 status did not exclusively determine the anti-HIV-1 potency, we set out to identify a

proteomic profile that defines the anti-HIV-1 potency of the CMPs. We imputed the cumulative AUCs of each sample against all the viruses to cluster them into two groups, independent of the donor's HIV status, using the Wilcoxon–Mann–Whitney test. Clustering resulted in group 1 displaying a significantly lower cumulative AUC mean compared with group 2, reflecting the differential

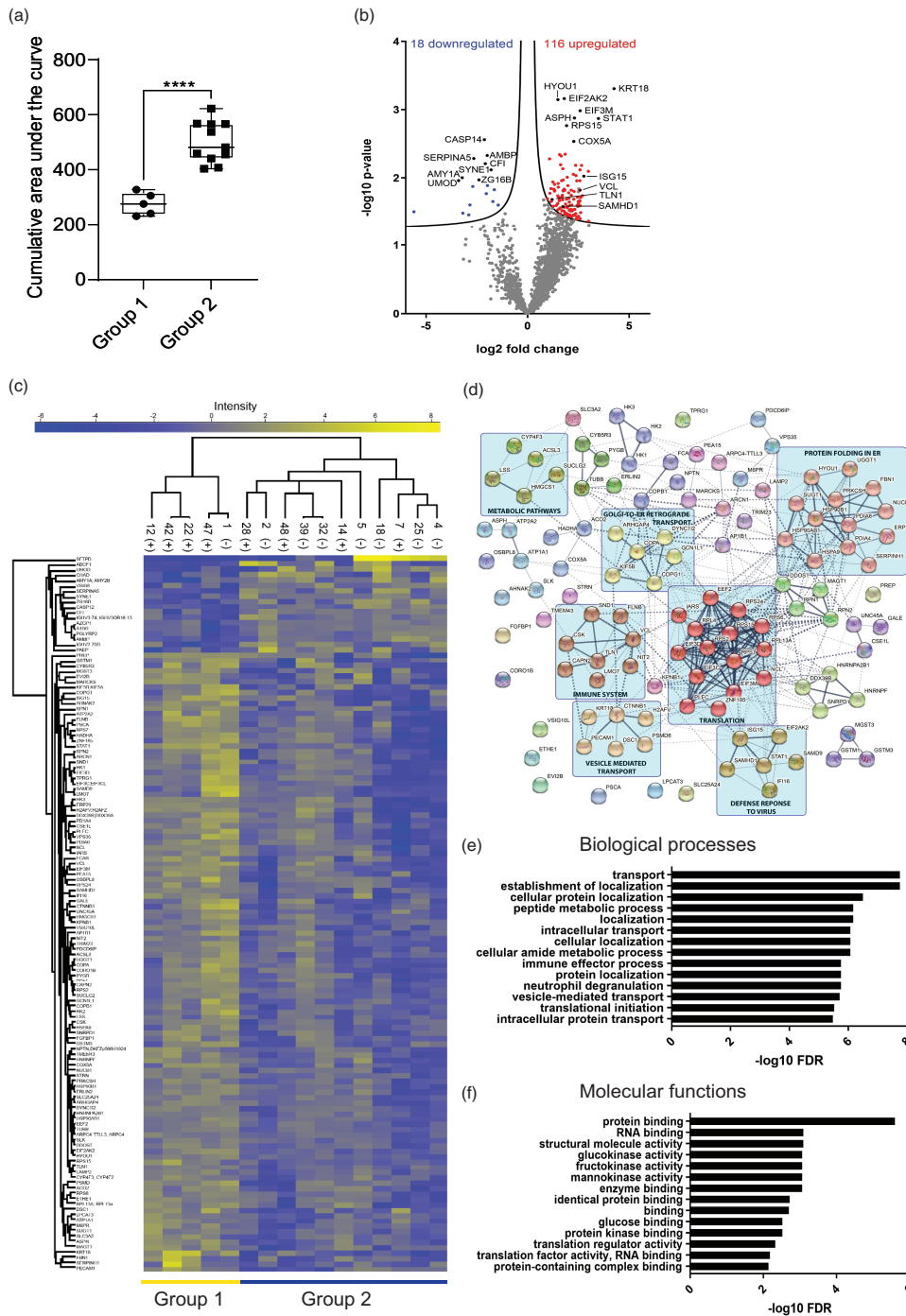


Fig. 5. Proteomic profiling of the potent and nonpotent cervical mucus plugs against HIV-1 infection. (a) Wilcoxon–Mann–Whitney test analysis of the potent (1) and less potent (2) CMPs against HIV-1 strains in the context of cell-free infection using the cumulative area under the curve values. (b) Volcano plot showing the significantly upregulated (116) and downregulated (18) proteins in the CMPs in groups 1 and 2. The statistical P value ($-\log_{10} P$) is plotted against the LFQ intensity difference (\log_2). (c) Heatmap analysis of the significantly regulated proteins between the CMPs from groups 1 and 2, following an unsupervised hierarchical clustering. (d) STRING analysis showing the diverse protein–protein interactions between significantly upregulated proteins in group 1. The network is displayed after MCL clustering (inflation parameter 3) and functional enrichment analysis of proteins within each cluster, with seven largest clusters encircled and annotated by their main description. Full lines demonstrate interactions within a cluster and dotted lines demonstrate interactions outside the clusters. Line thickness corresponds to STRING edge confidence. Gene ontology (GO) functional enrichment analysis of the significantly upregulated proteins; (e) GO term biological process and (f) GO term molecular function. The functional enrichments provided by STRING analysis are plotted according to their $-\log_{10}$ transformed false discovery rate (FDR). CMPs, cervical mucus plugs.

anti-HIV-1 potency (Fig. 5a). Statistical comparison based on this anti-HIV-1 potency grouping (Supplementary Data File 2, <http://links.lww.com/QAD/C228>) showed 116 and 18 proteins that were upregulated and downregulated, respectively, in group 1 (Fig. 5b). Strikingly, among significantly upregulated proteins in group 1 was the well characterized HIV-1 restriction factor SAMHD1 [37].

An unsupervised hierarchical clustered heatmap of differentially expressed proteins showed distinct proteomic profiles between the two groups (Fig. 5c). STRING analysis of 116 upregulated proteins in group 1 showed a heavily connected network of proteins, which displayed protein clusters that can potentially drive an anti-HIV-1 response (Fig. 5d). Among the top 14 biological processes (Fig. 5e) attributed to the 116 proteins are immune effector process and neutrophil degranulation, which are part of the antiviral host responses. Molecular functions (Fig. 5f) attributed to the 116 proteins include the translational machinery and glycolysis. Collectively, a distinct proteomic profile defines the differential anti-HIV-1 potency of the CMPs.

Discussion

Studies of the protection of the FRT against HIV-1 infection largely focused on cervicovaginal fluid [38–41]. The protective properties of the CMP in the cervix are because of its antimicrobial factors [8,9,19] and viscous nature through the gel-forming properties of its mucins [1,10,42]. A previous study reported that the CMPs, from self-declared HIV-negative donors, did not inhibit HIV-1 in an in-vitro assay but its purified mucins did [21]. We revisited this topic and found that the CMPs from HIV-1-negative and HIV-1-positive donors inhibited a panel of replication-competent SIV and HIV-1 strains more potently than the purified mucins, and a specific proteomic profile defines this antiviral potency. Therefore, we attribute these discrepancies to their use of one HIV-1 strain and qualitative p24 antigen assay as a readout. Our study was broad in terms of sample size, viruses and experiments; and found consistent antiviral activities across different quantitative readouts.

The CMPs from both cohorts displayed a potent antiviral activity and strain-specific pro-viral activity (Fig. 1a and b), suggesting a degree of heterogeneity that is independent of the donor's HIV-1 status. The potent anti-HIV-1 activity of the CMPs from the HIV-1-positive cohort (Fig. 1c) suggests the potential shedding of anti-HIV-1 factors into these samples. Enhanced potency against X4-tropic strains (Fig. 1d) is reminiscent of the well known selective transmission of R5-tropic viruses during heterosexual transmission [43–45]. How the CMPs collected in labour compare with those that are

found during gestation in the context of HIV-1 inhibition will likely depend on the gestational stage, given the gradual maturation of the CMP from early pregnancy to term [46].

In agreement with Habte *et al.* [21], purified cervical mucins inhibited HIV-1 in a dose-dependent manner, irrespective of the donor's HIV-1 status and viral tropism (Supplementary Fig. 3a and b, <http://links.lww.com/QAD/C223>). The mucins from the HIV-1-positive cohort also showed enhanced HIV-1 inhibition (Supplementary Fig. 3c, <http://links.lww.com/QAD/C223>), possibly through an altered glycosylation profile that could enhance mucin-virus interactions. Future studies should include glycome profiling of the mucins from both cohorts to unravel this potential phenomenon. The enhanced susceptibility of R5-tropic HIV-1_{Ba-L} to inhibition by the purified mucins compared with X4-tropic HIV-1_{NL4.3} (Supplementary Fig. 3d, <http://links.lww.com/QAD/C223>), challenges the proposal that the electrostatic interactions between the mucins and the V3 loop of gp120 among the X4-tropic strains drive the sieve effect reported from the cervical mucus [43,47].

The potent inhibition of HIV-1_{NL4.3} by the CMPs during co-treatment (Fig. 2b) corroborates the barrier functions of the CMP, which are supported by its orientation *in vivo*, with its antimicrobial-rich cellular compartment facing the microbe-inhabited vaginal canal and the largely mucoid compartment facing the uterus [9,46], thus preventing pathogens from invading the foetomaternal unit and triggering preterm deliveries. The inhibition of fusion between HIV-1 and TZM-bl cells by certain CMPs (Fig. 2c–f) is likely because of inhibition of HIV-1 infection at the attachment level. The poor fusion inhibition from the purified mucins (Supplementary Fig. 4, <http://links.lww.com/QAD/C224>) corroborates their relatively mild anti-HIV-1 activity (Supplementary Fig. 3, <http://links.lww.com/QAD/C223>).

The CMPs largely phenocopied HIV-1-neutralizing antibodies [35], by potently inhibiting cell-free HIV-1_{NL4.3-GFP} (Fig. 3a and b) compared with cell-associated HIV-1_{NL4.3-GFP} (Fig. 3c and d), which partially subverted the anti-HIV-1 activity of the CMPs during cell-to-cell transmission (Fig. 3e). The more potent inhibition seen in the presence of efavirenz suggests that the GFP signal detected in the presence of the CMPs came from HIV-1 infection and not just potentially free-floating GFP that has disassociated from the virions. These data suggest that the CMPs largely exert virus-directed inhibition (Fig. 2b). The increased staining intensity of proteins of lower molecular weight in the CMPs on SDS-PAGE was observed in both cohorts (Fig. 4a). An upregulation of MUC5AC by HIV-1 infection has been reported [48], but not that of MUC1 and MUC6 (Fig. 4b). Interestingly, the downregulation of MUC21 in the HIV-1-positive

cohort provokes questions about its role in HIV-1 pathogenesis.

An upregulation of proteins with anti-HIV-1 activity – mucins [21,49], serpinA3 [50], siglec5 [51] and tetraspanins [52] – and possibly entrapped neutralizing antibodies and antiretroviral drugs in the CMPs, could contribute to the potent anti-HIV-1 activity seen among the CMPs from the HIV-1-positive cohort (Fig. 1c). The downregulation of PSGs among the HIV-1-positive mothers (Fig. 4b), which maintain maternal immune tolerance to the semi-allogenic foetal allograft [53], could explain the common pregnancy complications reported from this cohort [54]. Likewise, the downregulation of protein S with anticoagulant activity [55], provides insights into venous thromboembolic cases that are common among HIV-positive individuals [56–58]. Together, these data hint towards the possible molecular mechanisms underlying several disorders that are common among HIV-positive individuals, and provide a platform from which we can launch a search of solutions that could revolutionize the clinical care of HIV-positive individuals. Donor's HIV-1 status-based hierarchical clustering of the CMPs largely reflects the effect of HIV-1 infection on the proteome of the CMPs (Fig. 4c).

Complementation of the antiviral potency-based clustering of the CMPs with Wilcoxon–Mann–Whitney test ($P = 2.904e-06$) (Fig. 5a) sheds light on the proteomic profile that defines the antiviral potency of the CMPs (Fig. 5b and c). SAMHD1, ISG15, talin-1 and vinculin abundance was increased (Fig. 5b), and these proteins exhibit anti-HIV-1 activity [37,59,60]. Moreover, proteins that drive the cell's biosynthetic machinery, cellular amide metabolic process, translational initiation, immune effector function and glycolysis were upregulated in samples with high antiviral potency (Fig. 5d and f). This reflects metabolic plasticity, which is a phenotype exhibited by HIV-1-infected cells with enhanced anti-HIV-1 potential and natural control of infection [61]. Therefore, the proteomic profile of the CMPs in group 1 strongly supports their potent antiviral activity [37,60–62].

In conclusion, CMPs collected from HIV-1-negative and HIV-1-positive women exhibited a broad and heterogeneous anti-HIV-1 activity in the contexts of cell-free and cell-to-cell infections. This antiviral activity is associated with a specific proteomic profile, which was enriched with a spectrum of proteins that can directly and indirectly counteract HIV-1 infection.

Acknowledgements

We are grateful to Thomas Pietschmann for constant support and Daniel Todt for assisting with the plotting of

the dose–response curves. We thank the NIH AIDS Reagent Program for providing essential reagents. This work was supported by funding from the HZI, the Berlin Institute of Health (BIH) and the DFG SPP Priority Program 1923 'Innate Sensing and Restriction of Retroviruses', GO2153/4–2 grant to C.G. and the National Research Foundation (NRF) of South Africa to A.S.M. G.G. was supported by the Knut and Alice Wallenberg Foundation and the German Federal Ministry of Education and Research, together with the Ministry of Science and Culture of Lower Saxony through the Professorinnen Programm III. B.M. was funded by the Deutscher Akademischer Austauschdienst (DAAD), the National Research Foundation (NRF) of South Africa, the Poliomyelitis Research Foundation (PRF) and the Postgraduate Funding Office of the University of Cape Town.

Author's contributions: B.M., C.G. and A.S.M. designed research, performed experiments, analysed the data and wrote the article. A.L., A.P. and G.G. performed the LC-MS/MS experiments and data analysis. J.K. and F.K. conducted statistical analysis of the data. B.M., P.S., J.J., C.B.B., M.L.M. recruited the study participants and collected the cervical mucus plugs. All the authors reviewed the manuscript.

Conflicts of interest

There are no conflicts of interest.

References

1. Bansil R, Turner BS. **Mucin structure, aggregation, physiological functions and biomedical applications.** *Curr Opin Colloid Interface Sci* 2006; **11**:164–170.
2. Fahy JV, Dickey BF. **Airway mucus function and dysfunction.** *N Engl J Med* 2010; **363**:2233–2247.
3. Corfield AP. **Mucins: a biologically relevant glycan barrier in mucosal protection.** *Biochim Biophys Acta* 2015; **1850**:236–252.
4. Habte HH, Mall AS, de Beer C, Lotz ZE, Kahn D. **The role of crude human saliva and purified salivary MUC5B and MUC7 mucins in the inhibition of human immunodeficiency virus type 1 in an inhibition assay.** *Virology* 2006; **3**:99.
5. Habte HH, Kotwal GJ, Lotz ZE, Tyler MG, Abrahams M, Rodrigues J, *et al.* **Antiviral activity of purified human breast milk mucin.** *Neonatology* 2007; **92**:96–104.
6. Viergiver E, Pommerenke WT. **Measurement of the cyclic variations in the quantity of cervical mucus and its correlation with basal temperature.** *Am J Obstet Gynecol* 1944; **48**:321–328.
7. Wolf DP, Blasco L, Khan MA, Litt M. **Human cervical mucus. IV. Viscoelasticity and sperm penetrability during the ovulatory menstrual cycle.** *Fertil Steril* 1978; **30**:163–169.
8. Lee DC, Hassan SS, Romero R, Tarca AL, Bhatti G, Gervasi MT, *et al.* **Protein profiling underscores immunological functions of uterine cervical mucus plug in human pregnancy.** *J Proteomics* 2011; **74**:817–828.
9. Hein M, Petersen AC, Helmig RB, Uldbjerg N, Reinholdt J. **Immunoglobulin levels and phagocytes in the cervical mucus plug at term of pregnancy.** *Acta Obstet Gynecol Scand* 2005; **84**:734–742.
10. Lai SK, Wang YY, Wirtz D, Hanes J. **Micro- and macrorheology of mucus.** *Adv Drug Delivery Rev* 2009; **61**:86–100.

11. Becher N, Adams Waldorf K, Hein M, Ulldberg N. **The cervical mucus plug: structured review of the literature.** *Acta Obstet Gynecol Scand* 2009; **88**:502–513.
12. Freitas AC, Chaban B, Bocking A, Rocco M, Yang S, Hill JE, et al. **The vaginal microbiome of pregnant women is less rich and diverse, with lower prevalence of Mollicutes, compared to nonpregnant women.** *Sci Rep* 2017; **7**:9212.
13. Gipson IK, Ho SB, Spurr-Michaud SJ, Tisdale AS, Zhan Q, Torlakovic E, et al. **Mucin genes expressed by human female reproductive tract epithelia.** *Biol Reprod* 1997; **56**:999–1011.
14. Andersch-Bjorkman Y, Thomsson KA, Holmen Larsson JM, Ekerhovd E, Hansson GC. **Large scale identification of proteins, mucins, and their O-glycosylation in the endocervical mucus during the menstrual cycle.** *Mol Cell Proteomics* 2007; **6**:708–716.
15. Gipson IK, Spurr-Michaud S, Tisdale A, Menon BB. **Comparison of the transmembrane mucins MUC1 and MUC16 in epithelial barrier function.** *PLoS One* 2014; **9**:e100393.
16. Hanson RL, Hollingsworth MA. **Functional consequences of differential O-glycosylation of MUC1, MUC4, and MUC16 (downstream effects on signaling).** *Biomolecules* 2016; **6**:3.
17. Gipson IK, Spurr-Michaud S, Moccia R, Zhan Q, Toribara N, Ho SB, et al. **MUC4 and MUC5B transcripts are the prevalent mucin messenger ribonucleic acids of the human endocervix.** *Biol Reprod* 1999; **60**:58–64.
18. Gipson IK, Moccia R, Spurr-Michaud S, Argueso P, Gargiulo AR, Hill JA 3rd, et al. **The Amount of MUC5B mucin in cervical mucus peaks at midcycle.** *J Clin Endocrinol Metab* 2001; **86**:594–600.
19. Hein M, Valore EV, Helmig RB, Ulldberg N, Ganz T. **Anti-microbial factors in the cervical mucus plug.** *Am J Obstet Gynecol* 2002; **187**:137–144.
20. **World Medical Association Declaration of Helsinki: ethical principles for medical research involving human subjects.** *JAMA* 2013; **310**:2191–2194.
21. Habte HH, de Beer C, Lotz ZE, Tyler MG, Schoeman L, Kahn D, et al. **The inhibition of the human immunodeficiency virus type 1 activity by crude and purified human pregnancy plug mucus and mucins in an inhibition assay.** *Viol J* 2008; **5**:59.
22. Carlstedt I, Lindgren H, Sheehan JK, Ulmsten U, Wingerup L. **Isolation and characterization of human cervical-mucus glycoproteins.** *Biochem J* 1983; **211**:13–22.
23. Chirwa N, Mall A, Tyler M, Kavin B, Goldberg P, Krige JE, et al. **Biochemical and immunohistochemical characterisation of mucins in 8 cases of colonic disease—a pilot study.** *South Afr J Surg* 2007; **45**:18–23.
24. Laemmli UK. **Cleavage of structural proteins during the assembly of the head of bacteriophage T4.** *Nature* 1970; **227**:680–685.
25. Lodermeier V, Suhr K, Schrott N, Kolbe C, Sturzel CM, Krnavek D, et al. **90K, an interferon-stimulated gene product, reduces the infectivity of HIV-1.** *Retrovirology* 2013; **10**:111.
26. Stansell E, Desrosiers RC. **Fundamental difference in the content of high-mannose carbohydrate in the HIV-1 and HIV-2 lineages.** *J Virol* 2010; **84**:8998–9009.
27. Goffinet C, Michel N, Allespach I, Tervo HM, Hermann V, Krausslich HG, et al. **Primary T-cells from human CD4/CCR5-transgenic rats support all early steps of HIV-1 replication including integration, but display impaired viral gene expression.** *Retrovirology* 2007; **4**:53.
28. Cavrois M, De Noronha C, Greene WC. **A sensitive and specific enzyme-based assay detecting HIV-1 virion fusion in primary T lymphocytes.** *Nat Biotechnol* 2002; **20**:1151–1154.
29. Xu S, Ducroux A, Ponnurangam A, Vieyres G, Franz S, Musken M, et al. **cGAS-mediated innate immunity spreads intercellularly through HIV-1 Env-induced membrane fusion sites.** *Cell Host Microbe* 2016; **20**:443–457.
30. Jochim N, Gerhard R, Just I, Pich A. **Impact of clostridial glycosylating toxins on the proteome of colonic cells determined by isotope-coded protein labeling and LC-MALDI.** *Proteome Sci* 2011; **9**:48.
31. Cox J, Mann M. **MaxQuant enables high peptide identification rates, individualized p.p.b.-range mass accuracies and proteome-wide protein quantification.** *Nat Biotechnol* 2008; **26**:1367–1372.
32. Szklarczyk D, Gable AL, Lyon D, Junge A, Wyder S, Huerta-Cepas J, et al. **STRING v11: protein-protein association networks with increased coverage, supporting functional discovery in genome-wide experimental datasets.** *Nucleic Acids Res* 2019; **47** (D1):D607–d613.
33. Shimada K, Hayano M, Pagano NC, Stockwell BR. **Cell-line selectivity improves the predictive power of pharmacogenomic analyses and helps identify NADPH as biomarker for ferroptosis sensitivity.** *Cell Chem Biol* 2016; **23**:225–235.
34. Pinto D, Park YJ, Beltramello M, Walls AC, Tortorici MA, Bianchi S, et al. **Cross-neutralization of SARS-CoV-2 by a human monoclonal SARS-CoV antibody.** *Nature* 2020; **583**:290–295.
35. Abela IA, Berlinger L, Schanz M, Reynell L, Gunthard HF, Rusert P, et al. **Cell-cell transmission enables HIV-1 to evade inhibition by potent CD4bs directed antibodies.** *PLoS Pathogens* 2012; **8**:e1002634.
36. Agosto LM, Herring MB, Mothes W, Henderson AJ. **HIV-1-infected CD4+ T cells facilitate latent infection of resting CD4+ T cells through cell-cell contact.** *Cell Rep* 2018; **24**:2088–2100.
37. Hrecka K, Hao C, Gierszewska M, Swanson SK, Kesik-Brodacka M, Srivastava S, et al. **Vpx relieves inhibition of HIV-1 infection of macrophages mediated by the SAMHD1 protein.** *Nature* 2011; **474**:658–661.
38. Ghosh M, Fahey JV, Shen Z, Lahey T, Cu-Uvin S, Wu Z, et al. **Anti-HIV activity in cervical-vaginal secretions from HIV-positive and -negative women correlate with innate antimicrobial levels and IgG antibodies.** *PLoS One* 2010; **5**:e11366.
39. Anderson BL, Ghosh M, Raker C, Fahey J, Song Y, Rouse DJ, et al. **In vitro anti-HIV-1 activity in cervicovaginal secretions from pregnant and nonpregnant women.** *Am J Obstet Gynecol* 2012; **207**:65.e1–65.e10.
40. Nunn KL, Wang YY, Harit D, Humphrys MS, Ma B, Cone R, et al. **Enhanced trapping of HIV-1 by human cervicovaginal mucus is associated with lactobacillus crispatus-dominant microbiota.** *mBio* 2015; **6**:e01084–01015.
41. Tyssen D, Wang YY, Hayward JA, Agius PA, DeLong K, Aldunate M, et al. **Anti-HIV-1 activity of lactic acid in human cervicovaginal fluid.** *mSphere* 2018; **3**:4.
42. Leal J, Smyth HDC, Ghosh D. **Physicochemical properties of mucus and their impact on transmucosal drug delivery.** *Int J Pharm* 2017; **532**:555–572.
43. Margolis L, Shattock R. **Selective transmission of CCR5-utilizing HIV-1: the 'gatekeeper' problem resolved?** *Nat Rev Microbiol* 2006; **4**:312–317.
44. Zhu T, Mo H, Wang N, Nam DS, Cao Y, Koup RA, et al. **Genotypic and phenotypic characterization of HIV-1 patients with primary infection.** *Science* 1993; **261**:1179–1181.
45. van't Wout AB, Kootstra NA, Mulder-Kampinga GA, Albrecht-van Lent N, Scherpbier HJ, Veenstra J, et al. **Macrophage-tropic variants initiate human immunodeficiency virus type 1 infection after sexual, parenteral, and vertical transmission.** *J Clin Invest* 1994; **94**:2060–2067.
46. Becher N, Hein M, Danielsen CC, Ulldberg N. **Matrix metalloproteinases in the cervical mucus plug in relation to gestational age, plug compartment, and preterm labor.** *Reprod Biol Endocrinol* 2010; **8**:113.
47. Kwong PD, Wyatt R, Sattentau QJ, Sodroski J, Hendrickson WA. **Oligomeric modeling and electrostatic analysis of the gp120 envelope glycoprotein of human immunodeficiency virus.** *J Virol* 2000; **74**:1961–1972.
48. Gundavarapu S, Mishra NC, Singh SP, Langley RJ, Saeed AI, Feghali-Bostwick CA, et al. **HIV gp120 induces mucus formation in human bronchial epithelial cells through CXCR4/alpha7-nicotinic acetylcholine receptors.** *PLoS One* 2013; **8**:e77160.
49. Habte HH, de Beer C, Lotz ZE, Tyler MG, Kahn D, Mall AS. **Inhibition of human immunodeficiency virus type 1 activity by purified human breast milk mucin (MUC1) in an inhibition assay.** *Neonatology* 2008; **93**:162–170.
50. Aboud L, Ball TB, Tjernlund A, Burgener A. **The role of serpin and cystatin antiproteases in mucosal innate immunity and their defense against HIV.** *Am J Reprod Immunol* 2014; **71**:12–23.
51. Soto PC, Karris MY, Spina CA, Richman DD, Varki A. **Cell-intrinsic mechanism involving Siglec-5 associated with divergent outcomes of HIV-1 infection in human and chimpanzee CD4 T cells.** *J Mol Med (Berl)* 2013; **91**:261–270.
52. Sato K, Aoki J, Misawa N, Daikoku E, Sano K, Tanaka Y, et al. **Modulation of human immunodeficiency virus type 1 infectivity through incorporation of tetraspanin proteins.** *J Virol* 2008; **82**:1021–1033.

53. Moore T, Dveksler GS. **Pregnancy-specific glycoproteins: complex gene families regulating maternal-fetal interactions.** *Int J Dev Biol* 2014; **58** (2–4):273–280.
54. Xiao PL, Zhou YB, Chen Y, Yang MX, Song XX, Shi Y, et al. **Association between maternal HIV infection and low birth weight and prematurity: a meta-analysis of cohort studies.** *BMC Pregnancy Childbirth* 2015; **15**:246.
55. Hackeng TM, van 't Veer C, Meijers JC, Bouma BN. **Human protein S inhibits prothrombinase complex activity on endothelial cells and platelets via direct interactions with factors Va and Xa.** *J Biol Chem* 1994; **269**:21051–21058.
56. Rasmussen LD, Dybdal M, Gerstoft J, Kronborg G, Larsen CS, Pedersen C, et al. **HIV and risk of venous thromboembolism: a Danish nationwide population-based cohort study.** *HIV medicine* 2011; **12**:202–210.
57. Olson JJ, Schwab PE, Jackson J, Lange JK, Bedair HS, Abdeen A. **HIV-positive patients are at increased risk of venous thromboembolism after total joint replacement.** *J Am Acad Orthop Surg* 2020; **29**:479–485.
58. Matta F, Yaekoub AY, Stein PD. **Human immunodeficiency virus infection and risk of venous thromboembolism.** *Am J Med Sci* 2008; **336**:402–406.
59. Osei Kuffour E, Konig R, Haussinger D, Schulz WA, Munk C. **ISG15 deficiency enhances HIV-1 infection by accumulating misfolded p53.** *mBio* 2019; **10**:4.
60. Brown C, Morham SG, Walsh D, Naghavi MH. **Focal adhesion proteins talin-1 and vinculin negatively affect paxillin phosphorylation and limit retroviral infection.** *J Mol Biol* 2011; **410**:761–777.
61. Angin M, Volant S, Passaes C, Lecuroux C, Monceaux V, Dillies M-A, et al. **Metabolic plasticity of HIV-specific CD8+ T cells is associated with enhanced antiviral potential and natural control of HIV-1 infection.** *Nat Metab* 2019; **1**:704–716.
62. Ventoso I, Blanco R, Perales C, Carrasco L. **HIV-1 protease cleaves eukaryotic initiation factor 4G and inhibits cap-dependent translation.** *Proc Natl Acad Sci U S A* 2001; **98**:12966–12971.